LIMNOLOGY and OCEANOGRAPHY

ASLO

Limnol. Oceanogr. 9999, 2025, 1–17

doi: 10.1002/lno.70137

RESEARCH ARTICLE

How marine heatwaves are reshaping phytoplankton in the Northeast Pacific

Loïck Kléparski,[1*] **Clare Ostle**,[1] **Sonia D. Batten**,[2] **Nicolas Djeghri**,[3] **Claudine Hauri**,[4] **Rémi Pagès**,[4] **Suzanne Strom**[5]

[1]Continuous Plankton Recorder Survey, Marine Biological Association, Plymouth, UK; [2]North Pacific Marine Science Organization (PICES), Sidney, British Columbia, Canada; [3]Institut Universitaire Européen de la Mer, IUEM/UBO, Laboratoire des sciences de l'Environnement Marin, UMR 6539 LEMAR, Technopole Brest Iroise, Université de Brest, Plouzané, France; [4]International Arctic Research Center, University of Alaska Fairbanks, Fairbanks, Alaska, USA; [5]Shannon Point Marine Center, Western Washington University, Anacortes, Washington, USA

Abstract

In 2015 and 2019, the Northeast Pacific has undergone significant heatwave events that strongly disrupted marine ecosystems functioning and services. Here we use the data collected by the Continuous Plankton Recorder (CPR) survey to investigate the changes in summer phytoplankton abundance and morphology and show an increase in prolate (i.e., elongated) taxa during heatwave events, in response to warmer temperatures and declining nitrate. We also investigate the impacts of the morphological shifts on the carbon cycle and show that warmer periods were dominated by prolate cells with high carbon content, whereas cooler periods were dominated by oblate (i.e., flattened) cells with low carbon content. By altering community composition and the overall cells sinking velocity, these morphological shifts likely impacted the carbon cycle, as they were correlated with changes in surface chlorophyll *a* and particulate organic carbon concentrations.

The intensity and duration of marine heatwaves (MHWs) have increased in response to global climate change (Oliver et al. 2021). A MHW is defined as "a period of extreme (i.e., with a magnitude that significantly deviates from the typical conditions of a region) warm near-sea surface temperature (SST) that persists for days to months and can extend up to thousands of kilometres" (IPCC 2019; Oliver et al. 2021). They have major consequences for biological systems, such as increasing metabolic demands, reduction of food supply and reproduction failures (Smith et al. 2023). In 2015 and 2019, the Northeast Pacific underwent two major warming events known as the North Pacific Marine Heat Waves (NPMHWs; Supporting Information Fig. S1). The first, named the "warm blob" (which started in Winter 2013, reached the northern part of the Gulf of Alaska during Fall 2014 and lasted until 2016; Supporting Information Fig. S1) was caused by a teleconnection between the tropical and the extratropical Pacific and anomalous sea surface pressures that prevented ocean heat loss toward the atmosphere (Bond et al. 2015; Di Lorenzo and Mantua 2016; Scannell et al. 2020). The second, named the "blob 2.0," occurred during Summer 2019 and was related to a weakening of the North Pacific High-Pressure System that reduced wind induced mixing and evaporative cooling (Supporting Information Fig. S1; Amaya et al. 2020). More freshwater inputs from precipitation during this second heatwave also triggered a decline in salinity that enhanced water column stratification and confined the temperature anomaly in the near surface layers, further reinforcing the warming (Scannell et al. 2020). Such extreme MHWs events would not have been possible without the increase in atmospheric greenhouse gas concentrations (Barkhordarian et al. 2022) and were also both amplified by a weaker upwelling of cold waters caused by positive Northern Alaska

*Correspondence: loick.kleparski@hotmail.fr; loikle@mba.ac.uk

Associate editor: David Antoine

Data Availability Statement: Data are freely available (*see* Materials and methods section).

Gyre Oscillation (NGAO) phases (Hauri et al. 2024) as well as the occurrence of El Niño events (Di Lorenzo and Mantua 2016; Amaya et al. 2020).

North Pacific Marine Heat Waves had strong negative impacts on marine ecosystem functioning and services, with high socio-economic consequences, such as mass mortality events among marine mammals and birds, as well as declines among exploited fish, e.g., the Pacific cod *Gadus macrocephalus* (Barbeaux et al. 2020; Smith et al. 2021; Suryan et al. 2021; Jones et al. 2023). A decline in chlorophyll *a* (Chl *a*) concentration was also observed during the first NPMHW, together with an increase in the abundance of warm water planktonic species and a decrease in phytoplankton cell size over the continental shelves (Peña et al. 2019; Suryan et al. 2021; Batten et al. 2022). On the contrary, during the second MHW, an increase in abundance was documented in both large (e.g., diatoms; Batten et al. 2022) and small phytoplankton (e.g., *Synechococcus*; Cohen 2022). Through their impact on nutrient uptake capabilities, grazing resistance, and vertical motion (Litchman and Klausmeier 2008; Naselli-Flores and Barone 2011; Karp-Boss and Boss 2016; Naselli-Flores et al. 2021), and therefore the ecological niche sensu Hutchinson (i.e., the set of environmental conditions enabling a species to grow and reproduce; Hutchinson 1957), morphological traits are known to alter phytoplankton response to long term as well as seasonal climatic variability. For example, today in the North Atlantic, oblate (i.e., flattened) diatoms are mainly found in spring (when turbulence, viscosity and nutrients are high, but temperature is low), whereas prolate (i.e., elongated) diatoms are mainly found in summer (when turbulence, viscosity and nutrients are low, but temperature high; Kléparski et al. 2022). In the context of climate change, oblates are expected to decline while prolates are expected to increase (Kléparski et al. 2023). Such a shift in phytoplankton morphology has the potential to alter the biological carbon pump, i.e., the set of processes that transport organic carbon from the upper to the deep ocean (Mouw et al. 2016; Henson et al. 2022).

Although biological responses to MHWs are well documented, some underlying ecological mechanisms are still unclear. In this article, we investigate the changes in phytoplankton abundance and morphology that resulted from the NPMHWs and how they impacted the carbon cycles in the Northeast Pacific. By means of the data collected by the Continuous Plankton Recorder (CPR) survey, we first document an increase in summer prolate taxa abundance during the NPMHWs and demonstrate that this increase was related to warming SST and declining nitrate. Secondly, although we used average cell size and carbon content of each taxon, we reveal that between 2004 and 2021, warmer and cooler periods were associated with shifts in phytoplankton cell shape and potential carbon content, as well as surface Chl *a* and particulate organic carbon (POC) concentration, indicating that the changes in cell morphology likely altered the carbon cycle.

Materials and methods

Biological and environmental data

Plankton abundance

Data on phytoplankton and copepod abundance originated from the CPR survey. The CPR is a long-term plankton monitoring program that has sampled plankton in the North Pacific since 2000. Sampling is conducted between March and October on a monthly basis using a high-speed plankton recorder towed behind voluntary merchant ships, called "ships of opportunity," at a depth of ~ 7–10 m (Batten et al. 2003). Plankton are filtered by a 270 μm mesh silk and stored in a tank containing 4% formaldehyde preservative. Organisms are identified to a species level (when possible, otherwise only to genus) and abundance (for large copepods ≥ 2 mm) or semi-quantitative abundance (for small copepods < 2 mm and phytoplankton) are assessed. Copepods size limit (i.e., 2 mm) corresponds to the threshold used by CPR analysts to separate large and small organisms during the different CPR counting stages (Batten et al. 2003; Richardson et al. 2006). Phytoplankton and copepod abundances correspond, respectively, to a number of cells and individuals per CPR sample, which represents ~ 3 m^3 of seawater filtered (Jonas et al. 2004). Here we used the samples collected in the oceanic part of the Gulf of Alaska (i.e., from the region with a bathymetry greater than 500 m; Fig. 1) from 2004 to 2021, along the Anchorage-Tacoma (AT) route. This route was chosen because it is located within a homogeneous ecological area (i.e., the East Pacific Subarctic Gyres Province; Longhurst 1998), it benefits from a relatively high sampling effort and its trajectory has remained consistent since 2004. As the sampling by the CPR mainly occurs over the summer season, only samples collected between May and September were considered (i.e., a total of 1755 samples). The North Pacific CPR survey data can be obtained here: https://doi.mba.ac.uk/data/3086.

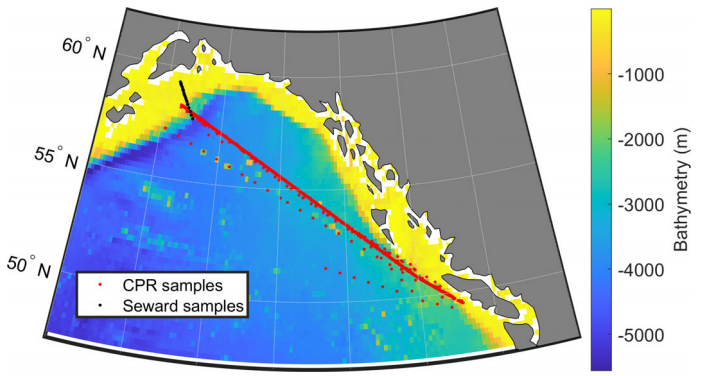

Fig. 1. Map of the Northeast Pacific and location of the Continuous Plankton Recorder (CPR) and Seward line samples. Continuous Plankton Recorder and Seward line sample locations are displayed by red and black dots, respectively. Colors denote the bathymetry (m).

Phytoplankton morphological traits

Data on phytoplankton mean cell carbon content (μg C cell^{-1}) were retrieved from the database gathered by Barton and colleagues (Barton et al. 2013) and completed with the data from the Global Diatom Database (Leblanc et al. 2012) for missing taxa. Data on dinoflagellates cell length and width were recovered from the Nordic Micro Algae website (http://nordicmicroalgae.org/) while diatom cell sizes (i.e., length/width/height, depending upon cell shape) were recovered from the Global Diatoms Database (Leblanc et al. 2012).

Following the method used by Kléparski and colleagues in the North Sea (Kléparski et al. 2022), diatom and dinoflagellate cell shapes were converted to cylinders and the corresponding mean cell heights and diameters were calculated based on both morphological and anatomical characteristics of the cells. For diatoms, their "original" geometric shapes are defined in the Global Diatoms Database as cylinder, cylinder + 2 half spheres, rectangular box, prism on elliptic base, prism on parallelogram base, cone + half sphere + cylinder, or prism on triangle base girdle view (Sun and Liu 2003). For diatoms with a cylindrical shape (e.g., cylinder, cylinder + 2 half spheres and cone + half sphere + cylinder), cell height (if not already characterized in the Global Diatoms Database) was defined as the dimension perpendicular to the cell diameter. For the other shapes, cell height was already defined in the Global Diatoms Database as the dimension perpendicular to the valves, representing an anatomic characteristic of the cells. The area of the slice perpendicular to cell height (as defined in the database) was therefore assessed and the diameter of the equivalent disk (i.e., the disk of equivalent surface) calculated. For *Ditylum brightwellii* (whose geometrical shape is defined as prism on triangle base girdle view), cell length was used as height. Cell diameters and heights were calculated based on minimum and maximum cell dimensions, and results were finally averaged. For dinoflagellates, cell width and length retrieved from the Nordic Micro Algae website were used as cell diameters and heights, respectively.

Cell shapes of each taxon were then characterized as oblate (i.e., mean cell diameter greater than or equal to mean cell height, flattened shape) or prolate (i.e., mean cell diameter smaller than mean cell height, elongated shape; Supporting Information Table S1). Previous studies have already used comparable groupings to explore how variations in cell morphology alter phytoplankton ecology and diversity (Karp-Boss and Boss 2016; Ryabov et al. 2021). Cell shape was also characterized by the height/diameter ratio (Supporting Information Table S1), which quantifies cell shape deviation from a sphere, a ratio smaller than 1 indicating cell flattening (i.e., oblate) while a ratio greater than 1 indicates cell elongation (i.e., prolate). Abundances collected by the CPR were also converted into biomass by multiplying the number of cells of each taxon in each CPR sample by the corresponding mean cell carbon content.

Gridded environmental data

Monthly SST (°C) originated from the ERA5 dataset and was downloaded from the Climate Data Store (accessed in September 2023; https://cds.climate.copernicus.eu/cdsapp#!/dataset/reanalysis-era5-single-levels?tab=overview).

Monthly mixed layer depth (MLD, m) originated from the ORAS5 dataset and was downloaded from the Climate Data Store (accessed in August 2023; https://cds.climate.copernicus.eu/cdsapp#!/dataset/reanalysis-oras5?tab=overview). The MLD is here defined as the depth of the ocean where the average sea water density exceeds the near surface density plus 0.01 kg m^{-3}. Mixed layer depth was used as a proxy for the wind induced turbulence.

Bathymetry (m) originated from the GEBCO Bathymetric Compilation Group (2019) and was obtained from the British Oceanographic Data Centre (BODC), National Oceanography Centre, NERC, United Kingdom (accessed in November 2019; https://www.bodc.ac.uk/data/published_data_library/catalogue/10.5285/836f016a-33be-6ddc-e053-6c86abc0788e/).

Monthly surface photosynthetically active radiation (PAR; einstein m^{-2} day^{-1}), Chl *a*, and POC concentration (mg m^{-3}) were downloaded from the Ocean Color website (accessed in February 2024; https://oceancolor.gsfc.nasa.gov/) and originated from observations of the Aqua-MODIS satellite. Particulate organic carbon was estimated based on remote sensing reflectance and the algorithm of Stramski and colleagues (Stramski et al. 2008), which exhibits strong predictive capacity (Evers-King et al. 2017).

Monthly nitrate and dissolved iron concentrations (mmol m^{-3}) were downloaded from the Copernicus Marine Services (CMEMS) and originated from the Global Ocean Biogeochemistry Hindcast (GLOBAL_REANALYSIS_BIO_001_029) dataset, which provides 3D biogeochemical fields along 75 depth levels for each variable since 1993 (accessed in May 2024; https://data.marine.copernicus.eu/product/GLOBAL_MULTIYEAR_BGC_001_029/description). Means were estimated for each variable along the first 10 m of the water column to fit with the CPR sampling depth.

All data were interpolated on a regular 0.25° grid (if not already provided on such a grid) and values of SST, MLD, bathymetry, PAR, Chl *a*, POC, nitrate, and dissolved iron concentration were attributed to each CPR sample (i.e., 1755 samples) by means of nearest neighbor interpolation (Wackernagel 1995). Annual SST anomalies were also estimated for the region from 45 to 65°N and from 160 to 120°W, based on the mean summer (i.e., May to September) SST between 2004 and 2021, to characterize regional temperature variability and MHWs locations between 2004 and 2021 (Supporting Information Fig. S1).

Non-gridded environmental data

The El Niño Southern Oscillation (ENSO) index was provided by the National Oceanic and Atmospheric Administration

(NOAA) Physical Sciences Laboratory, Boulder Colorado, USA (accessed in January 2024; https://www.psl.noaa.gov/enso/mei/). The index is estimated by means of an Empirical Orthogonal Function (EOF) on sea level pressure, SST, zonal and meridional components of the surface wind, and outgoing longwave radiation over the tropical Pacific basin (30°S–30°N and 100°E–70°W). Each EOF was calculated for 12 overlapping bi-monthly periods to consider ENSO seasonality and to reduce the effects of higher frequency intra-seasonal variability. The index provides an estimation of El Niño (positive index) and La Niña (negative index) events intensity. Annual averages were estimated based on summer indices to match our CPR samples, i.e., May–June, June–July, July–August, and August–September indices.

The Northern Gulf of Alaska Oscillation (NGAO) index was provided by the International Arctic Research Center, University of Alaska Fairbanks, Fairbanks, Alaska, USA (https://haurilab.alaska.edu/gulf-of-alaska/ngao-and-goadi). The index is based on an EOF of Sea Surface Heights (SSH) over the Gulf of Alaska (48.2°N–60°N and 163°W–133°W) and after removing the long-term temporal trend and deseasonalizing the data. The index describes the intensity of the upwelling in the Alaskan gyre, i.e., negative index values indicate a strong upwelling of cold, nutrient-rich, acidic, and deoxygenated waters, while positive index values indicate a weak upwelling (Hauri et al. 2021, 2024). Monthly means (from May to September) were averaged annually.

In situ size fractionated Chl *a* originated from the Seward line sampling program in the northern Gulf of Alaska (Fig. 1; Strom et al. 2016). Samples were collected during Spring and Fall in the upper 100 m of the water column via Niskin bottles. The size fractionated Chl *a* was assessed for two categories of phytoplanktonic organisms: micro ($> 20\,\mu$m) and nano ($< 20\,\mu$m) phytoplankton. Because of the existence of a strong cross-shelf gradient in phytoplankton and nutrients (Strom et al. 2006), monthly means were estimated for each category on the outer shelf (bathymetry < 500 m and from 147° and 149°W, so the stations closest to the shore were omitted) and in the open ocean (bathymetry ≥ 500 m). As size fractionated Chl *a* was not continuously assessed before 2011, monthly means were estimated between 2011 and 2021 for each May and September month (no sampling occurred between those 2 months), averaged at an annual scale (by considering all the May and September months for each year) and $\log_{10}$ transformed. Therefore, annual means only consider May and September months. To fit with the sampling depth of the CPR, only the samples collected between 0 and 10 m depth were used.

Numerical analyses

Data preparation

A total of 42 phytoplanktonic taxa were selected, as they were present in more than 10 CPR samples and information on mean cell sizes and cell carbon contents was available (Fig. 1; Supporting Information Table S1; note that we use the genus name of *Ceratium, as* referenced in the CPR database, instead of *Tripos*). The threshold of 10 CPR samples was chosen to remove rare and/or low abundant taxa that are not well sampled by the CPR. Some taxa with a high mean cell carbon content but observed in only one (or no) CPR samples along the AT route were therefore removed. Summer abundances and biomasses were averaged at a monthly scale (between May and September) for each taxon and missing values (i.e., 8 months on a total of 90 between 2004 and 2021, so less than 9%) were linearly interpolated by considering the abundances or biomass observed during the surrounding months (during the same year and the years before and after). Interpolated months were May 2008, June 2010, July 2008 and 2009, August 2015 and September 2004, 2009 and 2014. Finally, monthly summer means were averaged at an annual scale (by considering all the months between May and September for each year) and $\log_{10}(x + 1)$ transformed (Fig. 2; Supporting Information Figs. S2 and S3). These procedures were applied to reduce the variability usually observed in the planktonic data collected by the CPR survey (e.g., exceptional high abundance caused by local hydro-meteorological events, patchiness or the over-inflation of zero counts). To consider the spatio-temporal heterogeneity in the CPR sampling, summer monthly and annual means were also estimated for each environmental variable (except bathymetry) based on the same method and the values associated with each CPR sample by means of nearest neighbor interpolation, but without the $\log_{10}(x + 1)$ transformation (Fig. 3; Supporting Information Fig. S4). Therefore, environmental means are based on the same months (i.e., May to September) and years (i.e., from 2004 to 2021) as the CPR data.

Principal component analysis

Changes in phytoplankton abundance were characterized by means of a standardized principal component analysis (PCA) based on a correlation matrix of the mean annual summer abundance of the 42 taxa (i.e., 18 years by 42 taxa matrix; Supporting Information Figs. S2 and S3). Abundances were standardized (i.e., by subtracting the mean and dividing by the standard deviation; Legendre and Legendre 1998) so that all taxa had the same weight in the analysis. The resulting principal components (PCs) were also standardized by their maximum in absolute value for display purposes, and their significance tested by means of a broken stick test (Supporting Information Table S2; Legendre and Legendre 1998). Relationships between the changes in annual abundance of the 42 taxa and cell shapes (i.e., oblate or prolate) were investigated in the space defined by the first eigenvectors (Figs. 2 and 4). As the eigenvectors have been multiplied by the square root of the corresponding eigenvalues, they therefore describe the positive or negative correlation between the annual changes in abundance of each species and the corresponding PC (Legendre and Legendre 1998).

Consequently, when a species is located near 1 (−1) along one eigenvector, that species exhibits changes in abundance similar (opposite) to the corresponding PC. Hence, the aim of the PCA was to decompose the main trends in abundance exhibited by the 42 taxa and investigate their relationships with morphological traits (e.g., cell shape). K-means or other clustering algorithms could have been used here, but the PCA (ordination technique) was preferred because clustering methods require the choice of an arbitrary threshold to define different groups. Furthermore, PCAs have been widely applied on CPR data (Colebrook 1984, 1986; Beaugrand et al. 2003b) and a similar method has already been used to characterize the seasonal changes in oblate/prolate diatoms abundance in the North Sea (Kléparski et al. 2022). Changes in total mean annual relative and non-relative abundance and biomass (without the $\log_{10}(x+1)$ transformation) were also investigated by grouping oblate and prolate taxa (Fig. 2c–f).

Top-down vs. bottom-up mechanisms

Abundance data of 21 large (≥ 2 mm) and 15 small (< 2 mm) copepods were used to investigate the changes in grazing pressure and their impacts on phytoplankton abundance and morphology (Supporting Information Table S3). For the purposes of this analysis, we did not investigate dietary preferences of the copepod taxa and simply grouped them by size; however, predominantly carnivorous taxa are typically in low numbers compared to omnivorous or herbivorous taxa. The two size groups are known to exhibit distinct life history strategies, i.e., large copepods typically have one generation per year associated with an overwintering diapause phase, while small copepods typically have short generation times, so multiple generations per season. Therefore, the abundance of small copepods is more likely to respond quickly to any changes in environmental conditions, which explains why the two size classes have been found to exhibit distinct seasonal and long-term changes in abundance (Batten et al. 2018, 2022). As predator–prey interactions between phyto- and zooplankton occur at short time scales, monthly mean summer abundances were estimated for each copepod taxon by using the same procedure as for phytoplankton (*see* Data preparation section). Then, summer monthly averages were estimated for large and small copepods as well as for oblate and prolate phytoplankton. Pearson correlation coefficients between summer monthly changes in abundance of large, small copepods and oblate, prolate phytoplankton were then calculated. We assumed that negative correlations imply a top-down control such that copepod grazing pressure regulates phytoplankton abundance and morphology (e.g., high copepod abundances induce a higher grazing pressure so lower phytoplankton abundance are observed) while positive correlations imply a bottom-up control such that environmental changes regulate phytoplankton abundance and morphology (e.g., high phytoplankton abundance sustains high copepod abundance; Supporting Information Fig. S5).

Correlations between the first PCs and annual changes in summer SST, PAR, MLD, nitrate, and dissolved iron concentration, ENSO, and NGAO index were also assessed by means of Pearson correlation coefficients (Fig. 3; Table 1). Finally, a modeling approach was used to reconstruct the changes in phytoplankton abundances and investigate whether they were caused by the interaction between species ecological niches and the changes in environmental conditions (Supporting Information Text S1; Supporting Information Fig. S6).

Consequences on the carbon cycle

Changes in phytoplankton abundance and morphology were finally compared with changes in summer surface Chl *a* and POC concentrations. To do so, the long-term changes in mean cell carbon content and height/diameter ratio were quantified by means of a weighted average based on the abundance collected by the CPR following:

$$A_j = \frac{\sum_1^n x_i w_{ij}}{\sum_1^n w_{ij}} \quad (1)$$

With A_j the weighted mean for cell carbon content or height/diameter ratio for year j, x_i the mean cell carbon content ($\log_{10}$ transformed) or height/diameter ratio of taxa i, w_{ij} the mean summer abundance of taxa i for year j (without the $\log_{10}(x+1)$ transformation) and n the total number of taxa (i.e., 42). Therefore, annual changes in mean cell carbon content and height/diameter ratio do not consider the intraspecific morphological plasticity exhibited by phytoplanktonic cells in response to warming (Atkinson et al. 2003; Peter and Sommer 2012). Correlation between the changes in carbon content, height/diameter ratio and annual changes in surface Chl *a* and POC concentrations from the Aqua-MODIS satellite, size fractionated Chl *a* along the Seward line, ENSO and NGAO indices were assessed by means of Pearson correlations coefficients (Fig. 5; Table 2).

Results

Shifts in phytoplankton abundance and morphology

A PCA was applied on the mean annual summer abundances of the 42 phytoplanktonic taxa (i.e., 18 years by 42 taxa matrix) collected by the CPR survey along the AT route, to investigate the relationship between the changes in abundances and cell shapes (Supporting Information Table S1; Supporting Information Figs. S2 and S3). The broken stick test revealed that the first two PCs were significant; although other PCs were significant, only the first two were retained here because they explained ~ 30% of the total variance (Supporting Information Table S2) and almost all taxa were well represented in that space (*see* the circle of equilibrium contribution in Fig. 2b). The first PC (PC1; 19.54% of the total variance) exhibited positive values between 2004 and

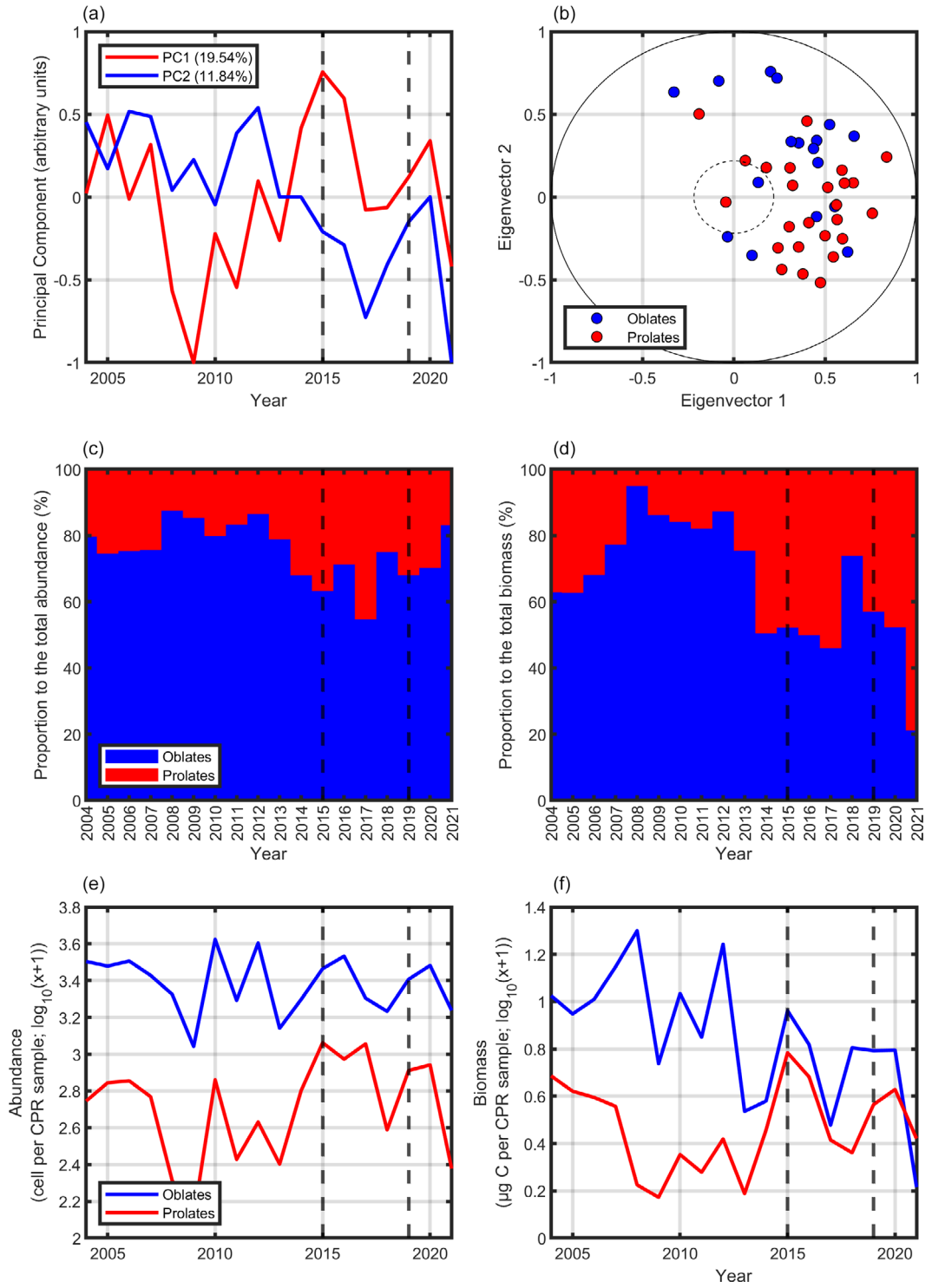

Fig. 2. Changes in oblate and prolate summer abundance and biomass. (**a**) Standardized principal component analysis (PCA) realized on the mean annual summer abundance of 42 taxa (*see* Supporting Information Table S1 and Figs. S2 and S3) between 2004 and 2021 in the oceanic part of the Northeast Pacific. First and second principal components (PCs) are displayed by red and blue lines, respectively. Percentages of variance explained by each PC are displayed in the panel legend. (**b**) Relationship between the first two eigenvectors and phytoplankton cell shape. The circles of correlation and of equilibrium contribution are displayed as a solid and a dashed line, respectively. Taxa located outside the circle of equilibrium contribution are significantly contributing to the corresponding PC. Changes in oblates and prolates mean annual relative summer (**c**) abundance and (**d**) biomass. Changes in oblates and prolates mean annual summer (**e**) abundance and (**f**) biomass ($\log_{10}(x + 1)$ transformed). In b–f, oblates and prolates are in blue and red, respectively. Vertical dashed black lines in (**a**), (**c**), (**d**), (**e**) and (**f**) indicates the timing of the North Pacific Marine Heatwaves (i.e., 2015 and 2019).

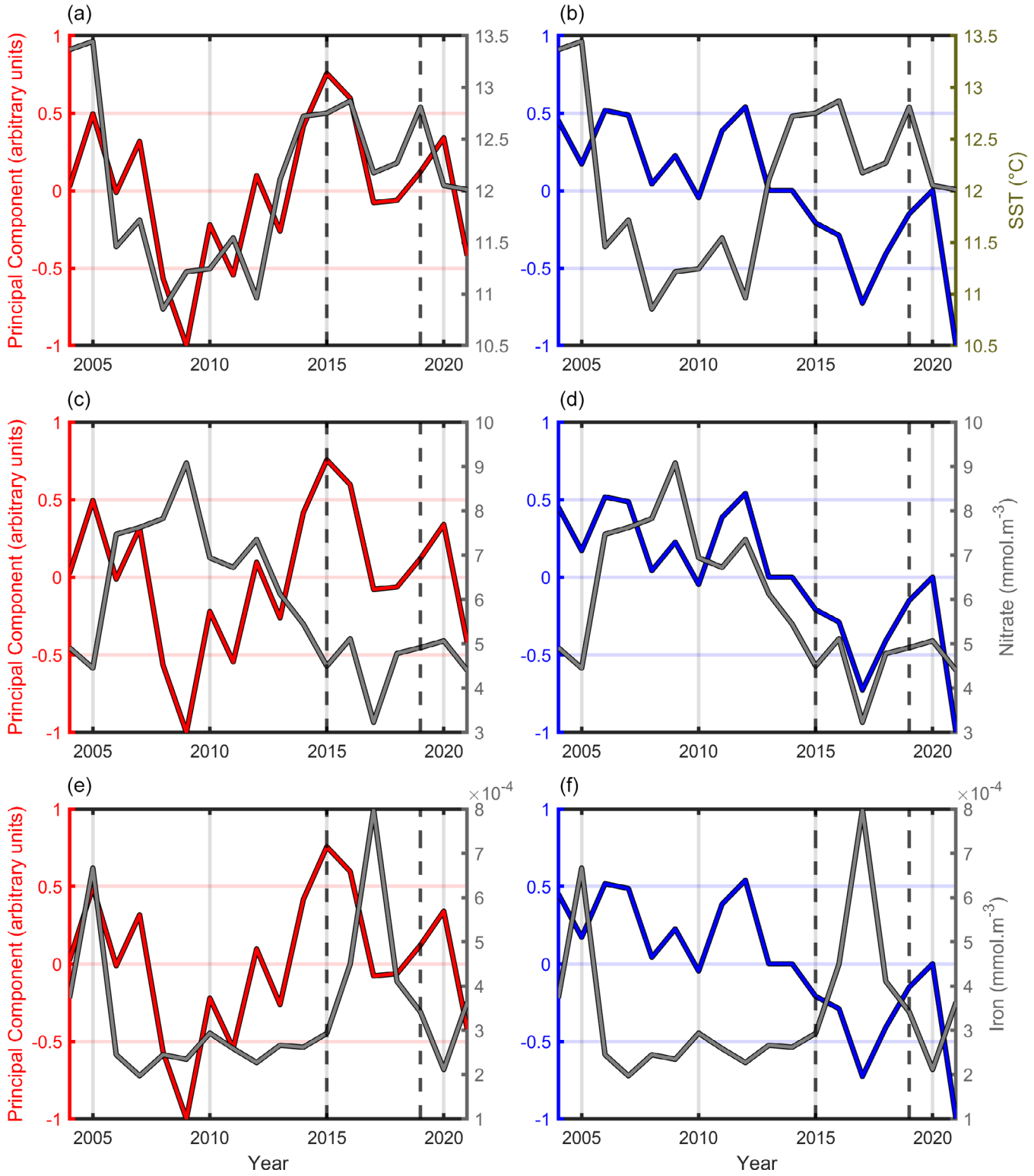

Fig. 3. Relationships between the first principal components (PCs) and the long-term changes in mean annual summer sea surface temperature (SST), nitrate and iron. In each panel, PCs are displayed along the left axis and long-term changes in SST, nitrate, and iron along the right axis. PC1 is displayed by red lines, PC2 by blue lines, and the long-term changes in SST, nitrate, and iron by gray lines. Relationship between (**a**) PC1 and SST, (**b**) PC2 and SST, (**c**) PC1 and nitrate, (**d**) PC2 and nitrate, (**e**) PC1 and iron, and (**f**) PC2 and iron. Vertical dashed black lines indicate the timing of the North Pacific Marine Heatwaves (i.e., 2015 and 2019). Correlations between each PC and the different environmental variables are displayed in Table 1.

Table 1. Pearson correlation coefficients between the first and second principal component (PC1 and PC2) and annual changes in summer environmental parameters and climatic indices. Pearson correlation coefficients between each PC and long-term changes in summer sea surface temperature (SST), photosynthetically active radiation (PAR), mixed layer depth (MLD), nitrate and dissolved iron concentrations, El Niño Southern Oscillation (ENSO) and Northern Gulf of Alaska Oscillation (NGAO) index are displayed in the second to last column, respectively. Bold numbers highlight significant correlations at $p < 0.05$. Long-term changes of each environmental variable are displayed in Fig. 3 and Supporting Information Fig. S4.

	SST	PAR	MLD	Nitrate	Dissolved iron	ENSO	NGAO
PC1	**0.63**	0.36	0.10	**−0.52**	0.20	**0.41**	**0.76**
PC2	−0.22	−0.23	−0.08	**0.65**	**−0.49**	0.15	−0.05

2007, 2014 and 2016, and 2019 and 2020 (Fig. 2a). The second PC (PC2; 11.84% of the total variance) exhibited positive values from 2004 to 2014, followed by a period of negative values until 2021 (Fig. 2a). Among the 42 taxa, 17 were identified as oblates (only diatoms except the dinoflagellates *Cladopyxis* spp.) and 25 as prolates. Cell shapes of some known "elongated" diatoms were characterized as oblates because of their small cell height (defined as the dimension perpendicular to the valves; *see* Materials and methods), i.e., *Thalassiothrix longissima*, *Pseudo-nitzschia delicatissima* and *seriata* complex, *Nitzschia/Pseudo-nitzschia* spp., *Thalassionema nitzschioides*, *Fragilaria* spp., and *Cylindrotheca closterium* (i.e., 7 taxa out of 42, so less than 17% of all species).

Relationships between the changes in mean annual summer abundance and cell shapes were examined in the space defined by the first two eigenvectors, which described the correlations between the first/s PCs and the annual changes in abundance of the 42 taxa (Fig. 2a,b; Supporting Information Figs. S2 and S3). Results showed that the taxa positively correlated with PC1 and negatively with PC2 (indicating an increase of their abundance during the NPMHWs) were mainly prolates (Fig. 2b). On the contrary, taxa positively correlated with PC2 but not with PC1 (indicating a decrease of their abundance during the NPMHWs) were mainly oblates (Fig. 2b). The study of the changes in mean annual summer relative abundance and biomass confirmed an increase in prolate taxa during the NPMHWs, which reached values close to 40% of the total abundance and 50% of the total biomass collected by the CPR during the NPMHWs (Fig. 2c,d). While the relative abundance of prolates declined after 2017, their relative biomass strongly increased after that time, reaching values greater than 70% of the total biomass collected by the CPR in 2021 (Fig. 2d). On the contrary, oblate relative abundance exhibited a decline between 2012 and 2017 (from 87% to 55%), followed by an increase until 2021, while their relative biomass exhibited a sharp decline from 2014 to 2021, except in 2018, where it returned to pre-heatwave levels (Fig. 2c,d). Changes in mean non-relative abundance and biomass also confirmed prolates increased, but they also showed that oblate abundance has remained important and even higher than prolate abundance throughout the period 2004–2021 (Fig. 2e), while their biomass collapsed in 2021, therefore indicating a shift toward smaller oblate cells (and explaining the sharp increase in prolate relative biomass for that year; Fig. 2f).

No significant correlations were found between the changes in large copepod summer abundance and the two phytoplanktonic groups, but weak positive correlations were found between the monthly changes in small summer copepods and both oblates and prolates ($r_{Pearson} = 0.32$ and 0.25, respectively; Supporting Information Fig. S5). These results suggested a bottom-up control and therefore that the changes in summer phytoplankton abundance and morphology were related to environmental changes and not to a shift in copepod grazing pressure (*see* Materials and methods). This assumption was confirmed by significant correlations between PC1 and the annual changes in summer SST ($r_{Pearson} = 0.63$) and nitrate ($r_{Pearson} = -0.52$), and also between PC2 and the annual changes in summer nitrates ($r_{Pearson} = 0.65$) and dissolved iron ($r_{Pearson} = -0.49$; Fig. 3; Table 1). Significant positive correlations were also found between PC1 and the ENSO and NGAO indices ($r_{Pearson} = 0.41$ and 0.76, respectively; Table 1). No significant correlations were found with summer MLD and PAR (Supporting Information Fig. S4). Finally, a modeling approach demonstrated that the changes in summer phytoplankton abundance were well explained by bottom-up mechanisms alone, i.e., the interaction between species ecological niches (i.e., their environmental requirement) and the interannual changes in SST and nitrates (Supporting Information Text S1; Supporting Information Fig. S6).

A synthesis of the changes in oblate and prolate phytoplankton and how they relate to the changes in summer temperature and nutrients is shown in Fig. 4, which displays each taxon in the space defined by the first two eigenvectors as a cylinder scaled with the corresponding mean cell height and diameter. Figure 4 confirmed that the taxa positively correlated with PC1 and negatively with PC2 (i.e., taxa that increased during the NPMHWs) were mainly large prolate diatoms and dinoflagellates (e.g., *Proboscia alata* and *Ceratium horridum*). In contrast, the taxa positively related to PC2 (i.e., taxa that decreased during the NPMHWs) were mainly oblate diatoms and small compact dinoflagellates

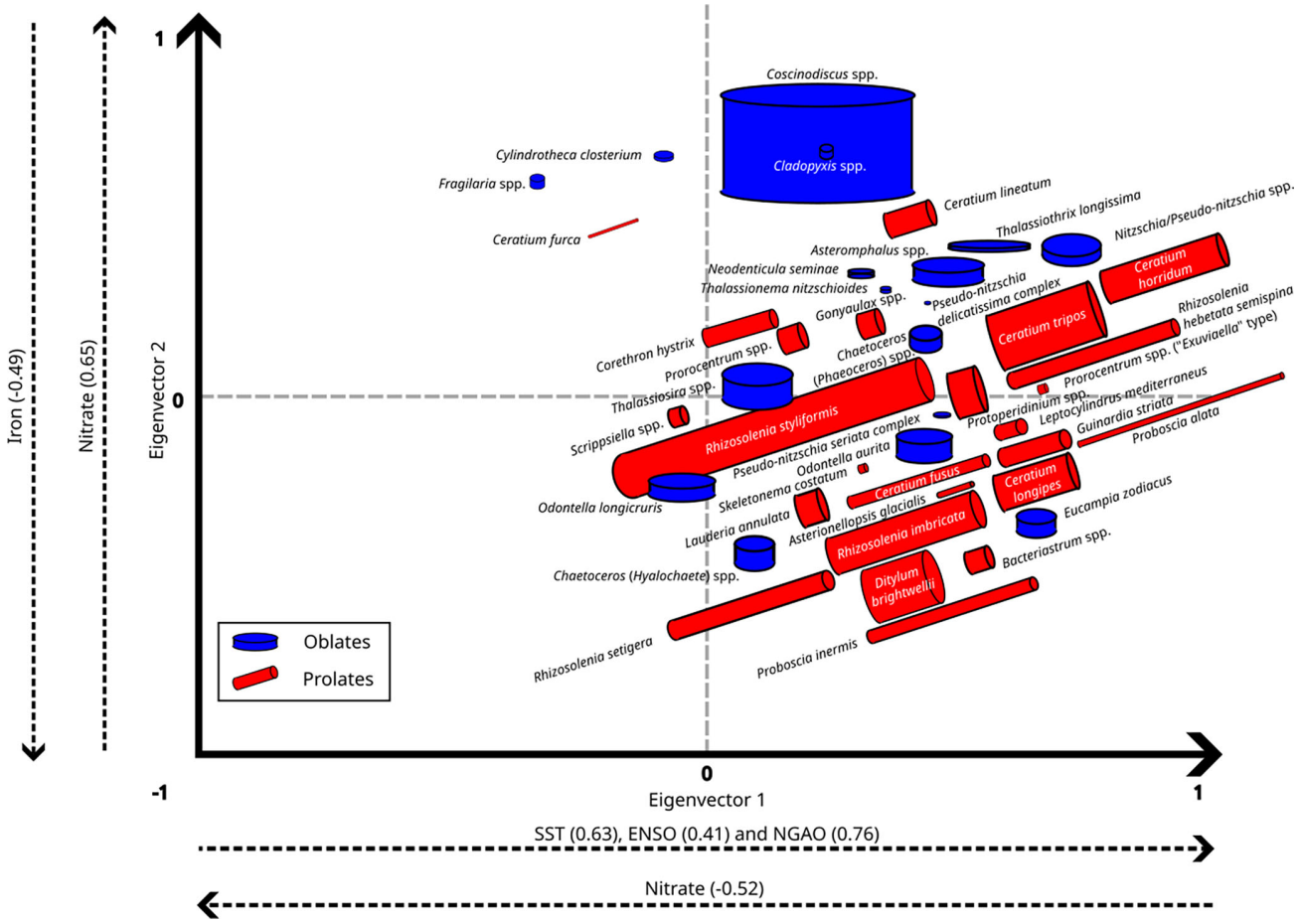

Fig. 4. Summary of the relationship between the first two eigenvectors, changes in oblates and prolates summer abundance, and the environment. Cell shapes are represented by cylinders scaled with taxa mean cell height and diameter (Supporting Information Table S1). Oblates and prolates are in blue and red, respectively. Changes in summer environmental parameters and climate indices are displayed by the dashed arrows (correlations between PC1-2 and the different environmental variables are displayed into brackets and in Table 1). Taxon names are those recorded in the Continuous Plankton Recorder (CPR) database.

(e.g., *Coscinodiscus* spp. and *Cladopyxis* spp.). Few exceptions were observed with very small and compact taxa, such as *Prorocentrum* spp. ("*Exuviaella*" type) and *Eucampia zodiacus*, positively correlated with PC1 or the thin elongated dinoflagellates *Ceratium furca* positively related to PC2 (Fig. 4).

Impacts on the carbon cycle

Significant correlations between the changes in mean cell carbon content, height/diameter ratio, climatic and biogeochemical indices further revealed that positive ENSO (i.e., El Niño) and positive NGAO periods (i.e., weak cold water upwelling, so warmer periods associated with MHWs; 2004–2006, 2014–2015 and 2018–2019) were associated with an increase in summer abundance of high carbon, prolate taxa and a decline in surface summer Chl *a* and POC concentrations (Fig. 5a–c; Table 2). On the other hand, during cooler periods (i.e., negative ENSO and NGAO phases in 2007–2008, 2010–2013, 2016–2017 and 2020–2021), oblate taxa with low carbon content were more abundant, and surface summer Chl *a* and POC concentrations were higher (Fig. 5a–c; Table 2). No changes occurred during the positive ENSO of 2009, which could be because the NGAO was in a negative phase (i.e., strong cold-water upwelling; Fig. 5a). Shifts in summer Chl *a* and phytoplankton morphology were also confirmed by in-situ observations along the Seward line (Fig. 5d), although correlations with the changes in carbon content and height/diameter ratio were not significant (Table 2), and the spatial coverage of the Seward line is reduced in comparison (Fig. 1). Seward observations suggested an increase in the contribution of nano (i.e., small) phytoplankton (< 20 μm) to the total summer Chl *a* concentration during MHWs, positive ENSO, and NGAO, while the contribution of micro (i.e., larger) phytoplankton increased during cooler periods (i.e., negative ENSO and NGAO; Fig. 5d). Similar changes in nano and micro phytoplankton were also observed on the shelf (Supporting Information Fig. S7).

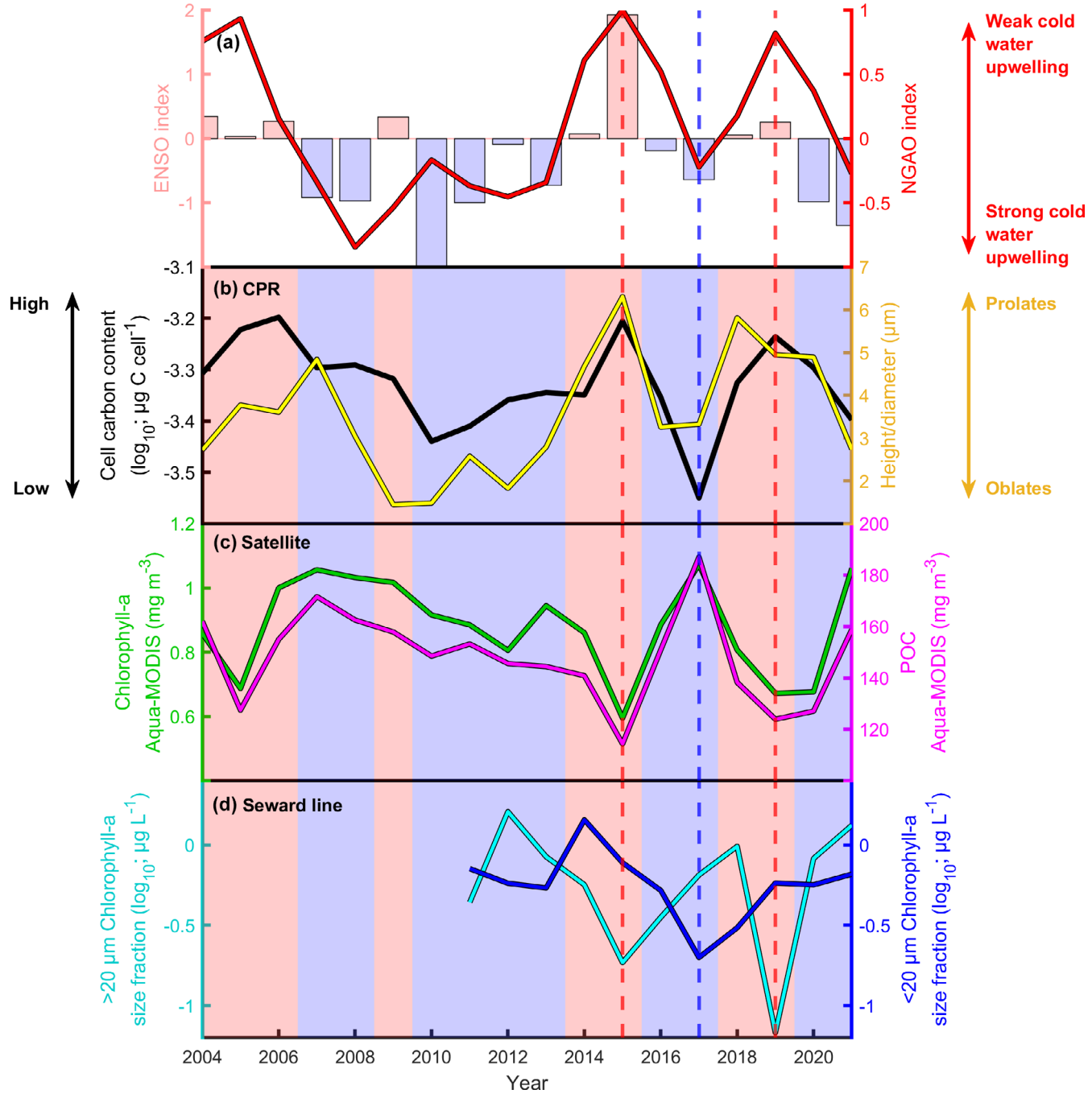

Fig. 5. Relationships between morphological changes and the carbon cycle. (**a**) Long-term changes in summer El Niño Southern Oscillation (ENSO; red and blue bars, left axis) index and standardized summer Northern Gulf of Alaska Oscillation (NGAO) index (red line, right axis). Pale red and blue bars display positive and negative ENSO index, respectively. In (**b**), (**c**) and (**d**) pale blue and red backgrounds display the periods of negative and positive ENSO, respectively. Vertical dashed red lines indicate the timing of the North Pacific Marine Heatwaves (i.e., 2015 and 2019). The vertical dashed blue line indicates a period of relative cooling observed in 2017. (**b**) Long-term changes in mean cell carbon content ($\log_{10}$ transformed; black line, left axis) and mean height/diameter ratio (yellow line, right axis). High (low) cell carbon content indicates that large (small) cells are abundant, and high (low) height/diameter ratio that prolates (oblates) are increasing. (**c**) Long-term changes in chlorophyll *a* (green line, left axis) and particulate organic carbon (POC; magenta line, right axis) concentrations originating from Aqua-MODIS observations. (**d**) Long-term changes in more than 20 μm ($\log_{10}$ transformed; cyan line, left axis) and less than 20 μm ($\log_{10}$ transformed; blue line, right axis) chlorophyll *a* size fraction along the oceanic part of the Seward line.

Table 2. Pearson correlation coefficients between annual changes in mean summer cell carbon content, height/diameter ratio, summer environmental parameters and climatic indices. Pearson correlation coefficients between annual changes in mean summer cell carbon content, height/diameter ratio and long-term changes in summer chlorophyll *a* (Aqua-MODIS), particulate organic carbon (POC; Aqua-MODIS) concentrations, more than 20 μm ($\log_{10}$ transformed) and less than 20 μm ($\log_{10}$ transformed) chlorophyll size fraction along the oceanic part of the Seward line, El Nino Southern Oscillation (ENSO) index and Northern Gulf of Alaska Oscillation (NGAO) index are displayed in the second to last column, respectively. Bold numbers highlight significant correlations at $p < 0.05$.

	Chlorophyll *a* Aqua-MODIS	POC Aqua-MODIS	> 20 μm chlorophyll size fraction	< 20 μm chlorophyll size fraction	ENSO	NGAO
Mean cell carbon content	**−0.50**	**−0.61**	−0.51	0.48	**0.59**	**0.48**
Height/diameter	**−0.52**	**−0.50**	−0.48	0.07	**0.48**	**0.58**

Discussion

Phytoplanktonic cells exhibit a large diversity of sizes and shapes, from simple cylindrical ones, such as *Coscinodiscus* spp., to more complex shapes, such as *C. horridum*. Various standardized geometric models have therefore been developed to estimate cell biovolume (Hillebrand et al. 1999; Sun and Liu 2003). However, there is always a dilemma on whether one should use simple and easily measurable models or more complex ones close to true natural shapes (Sun and Liu 2003). Here, diatom and dinoflagellate shapes have been simplified by assimilating them to cylinders, an assumption that has some limitations with, for example, some elongated taxa such as *T. longissima* being identified as oblates. However, this procedure has already been successfully applied in the North Atlantic to investigate long-term as well as seasonal changes in phytoplankton abundance and morphology (Kléparski et al. 2022, 2023). Furthermore, by doing so, shape attribution was not based on a series of subjective choices, but instead on true anatomic features of the cells (because cell heights are already described in the database) at least for diatoms (*see* Materials and methods). For dinoflagellates, as no height or diameter was clearly defined in the original database (i.e., the Nordic Micro algae website), we decided to use cell width and length as diameter and height, respectively. For some taxa, such as *C. horridium*, that exhibit a complicated shape which is hard to categorize, this can be seen as an oversimplification. However, by doing so, all dinoflagellates were characterized as prolates (except *Cladopyxis* spp.), which is consistent with the ecology of that group (i.e., dinoflagellates and prolate diatoms have been found to exhibit similar seasonal and long-term changes in abundance; Kléparski et al. 2023).

In the context of global climate change, it is usually assumed that a warmer ocean will induce a shift toward smaller phytoplanktonic taxa better adapted to stratified low nutrient conditions and to an enhanced copepod grazing pressure on larger cells (Bopp et al. 2005; Lewandowska and Sommer 2010; Marinov et al. 2010). However, although small taxa such as *Skeletonema costatum* or *E. zodiacus* have increased during the NPMHWs (Fig. 4; Supporting Information Figs. S2 and S3), as well as the contribution of nano phytoplankton to the total summer Chl *a* concentration (Fig. 5d), our results based on summer CPR data demonstrate that warming events and declining nitrate in the oceanic part of the Northeast Pacific have likely induced an increase in large prolate cells (Figs. 2–4; Supporting Information Text S1; Supporting Information Fig. S6). Such an increase in response to global climate change had already been suggested from a model associated with CPR data in the North Atlantic, where an increase in prolate diatoms and dinoflagellates abundance is expected (Kléparski et al. 2023). Hence, because the intensity and duration of MHWs are expected to increase (Oliver et al. 2021), together with the frequency of extreme El Nino events (Cai et al. 2014), our results provide insight into how the phytoplanktonic community might be reorganized in the coming decades.

Shifts in phytoplankton abundance and morphology can result either from (i) top-down control through changes in copepods grazing pressure or (ii) bottom-up control through, for example, a shift in nutrients and temperature (Smetacek 2001; Karp-Boss and Boss 2016; Hillebrand et al. 2022; Kléparski et al. 2022). Top-down controls are supposed to be enhanced during NPMHWs (Batten et al. 2022) and mesocosm experiments have demonstrated an enhanced grazing pressure in response to warming, especially during the post-bloom phase (Lewandowska and Sommer 2010; Lewandowska et al. 2014). However, the positive relationship between the monthly changes in zooplankton and phytoplankton summer abundance (Table 1; Supporting Information Fig. S5) indicates that changes in copepods grazing pressure have played a reduced role here. On the contrary, the positive correlations between PC1 and 2 and the environment (i.e., climatic indices, nutrients and temperature; Fig. 3; Table 1), as well as the results from the modeling approach (Supporting Information Text S1; Supporting Information Fig. S6), demonstrate that bottom-up processes were responsible for the observed increase in prolate abundance. Elongated cells are experiencing higher nutrients fluxes through their membrane (Pahlow et al. 1997; Karp-Boss and Boss 2016), which provide a competitive advantage under the low nitrate

conditions that were observed during the NPMHWs (Fig. 4a; Supporting Information Fig. S4). However, it has been suggested that lower nutrient supply during NPMHWs has a limited impact here (Wyatt et al. 2022) because of the nature of the Northeast Pacific, which is a High Nutrients Low Chlorophyll (HNLC) area where phytoplankton growth is permanently limited by low iron concentration (Martin et al. 1989). Cell elongation also provides an advantage in warmer, less viscous waters by decreasing cell sinking velocity because of the negative relationship between sea water viscosity and temperature (e.g., the sinking velocity of a 20 μm diameter cell will increase by 4% for each increase of 1°C; Smayda 1970). Therefore, a prolate cell would sink more slowly than an oblate one in low viscous warm waters. Furthermore, temperature also affects phytoplankton metabolism and resources (e.g., nutrients) allocation by decreasing the number of ribosomes in the cells but increasing the rate of protein synthesis (Toseland et al. 2013). As nitrate is a key constituent of proteins and nucleic acids (Miller 2004), this mechanism might also explain why prolate cells increased during the NPMHW: i.e., cell elongation enables prolates to remain in the well-lit upper part of the water column without affecting their ability to efficiently uptake nutrients (Padisak et al. 2003; Naselli-Flores and Barone 2011; Naselli-Flores et al. 2021; Kléparski et al. 2022).

The increase in summer abundance of prolate taxa with a lower sinking velocity would be expected to be associated with a reduced export of carbon during warming events, because of a higher remineralisation rate (Marsay et al. 2015). However, increasing CO_2 uptake has been observed during NPMHW periods (Duke et al. 2023) and in situ results in the northern Gulf of Alaska showed an enhanced export of carbon caused by phytoplankton cells aggregation during Summer 2019 (O'Daly et al. 2024). Furthermore, we observed a decline in surface POC concentration during positive ENSO-NGAO phases and MHW periods (Fig. 5a,c), which is thought to be related to an enhanced settling of large, fast sinking particles (Yu et al. 2019). One hypothesis to explain this apparent discrepancy would be a decoupling between phytoplankton production and the remineralisation process (Henson et al. 2019), such as the existence of short intense mixing events that would increase prolate cells sinking velocity as well as triggering an enhanced aggregate formation and thereby a higher carbon export (Clifton et al. 2018; Arguedas-Leiva et al. 2022). Geological records confirmed that warming events are associated with enhanced carbon export by diatoms in the Northeast Pacific (Lopes et al. 2015; Praetorius et al. 2015). A similar relationship has also been documented in the Mediterranean Sea, where the formation of sapropels is associated with high prolate diatom (i.e., rhizosolenid) export under stratified conditions (Kemp and Villareal 2013). Finally, the Northeast Pacific biological carbon pump can also be strengthened by the increase in dinoflagellate abundance. For example, it has been shown that dinoflagellate blooms were associated with strong carbon export at 3000 m in the Northeast Atlantic (Henson et al. 2012), while the implementation of a mixotrophic group (e.g., dinoflagellates) into a biogeochemical model has been shown to increase the flux of carbon exported toward depth (Ward and Follows 2016).

Comparison of the changes in mean cell carbon content, height/diameter ratio, and satellite observations showed that MHWs and positive ENSO-NGAO periods were associated with an increase of large prolate taxa and a decline in surface summer Chl *a* concentration (Fig. 5b,c). However, in situ observations along the Seward line showed a decline in the size fraction Chl *a* associated with large micro phytoplankton (> 20 μm), suggesting a decline of their abundance and an increase in smaller cells (< 20 μm; Fig. 5d). A decline in cell size and Chl *a* has already been documented on the northern continental shelves during the first MHW (Suryan et al. 2021), a result that is usually associated with a decline of the phytoplanktonic abundance and/or biomass (Behrenfeld et al. 2006; Boyce et al. 2010). Although the CPR is known to collect a consistent fraction of the in situ phytoplanktonic abundance, therefore reflecting the major changes that occurred at both seasonal and interannual scales, there is a bias toward recording larger organisms because of the mesh silk size used by the CPR (Richardson et al. 2006). Hence, part of the phytoplanktonic community (i.e., smaller cells) is under-sampled by the CPR, which can explain the apparent contradiction with the data collected along the Seward line. Furthermore, the contribution of smaller cells to total Chl *a* concentration is more important during MHWs periods (smaller cells sampled by the Seward program but not by the CPR; *see* Materials and Methods and Fig. 5d), and as those cells have a lower chlorophyll content (Hillebrand et al. 2022), this can explain the overall decline in surface Chl *a*. Hence, it would suggest that although high carbon prolate taxa increased during MHWs and positive ENSO-NGAO periods (as observed by the CPR), overall, the biomass of the entire phytoplanktonic community has declined (as observed along the Seward line). This discrepancy can also be related to the use of average cell sizes and carbon contents based on literature review (Leblanc et al. 2012; Barton et al. 2013) and not on actual in situ measurements (which would have been impractical here). Therefore, the intraspecific morphological plasticity usually observed in response to warming (i.e., reduce cell size) was not considered in our analyses (Atkinson et al. 2003; Peter and Sommer 2012). However, this mechanism may have a limited impact here, as results from a freshwater mesocosm suggested that shifts in community composition are more prevalent on community size spectrum than intraspecific morphological plasticity (Yvon-Durocher et al. 2011). Furthermore, contrasting responses to warming have been observed, with both cell size increase and decline being documented by different studies (Padfield et al. 2018; Hillebrand et al. 2022). Differences in the spatial extent of both CPR and Seward sampling programs can also explain the

discrepancy, i.e., the Seward data are located close to the shelf while CPR data are located in the open ocean (Fig. 1), which is also confirmed by the absence of significant correlations between the changes in mean cell carbon content, height/diameter ratio, and the Seward data (Table 2). Another explanation would be that surface Chl *a* concentration was altered by changes in phytoplankton intracellular pigmentation, a phenomenon known as photoacclimation and which has been shown to be an important component of chlorophyll temporal variability across the global ocean (Behrenfeld et al. 2005, 2016). By affecting water column stratification, nutrient concentrations, and light conditions (and therefore the relationship between phytoplankton growth and irradiance; Edwards et al. 2016), the changes in temperature are activating complex physiological pathways that regulate the intracellular chlorophyll synthesis (Behrenfeld et al. 2016). Hence, the changes in chlorophyll (satellite and along the Seward Line) may not reflect a proportional change in abundance but rather a change in intracellular pigmentation, which would tend to decline during MHW, positive ENSO, and positive NGAO. Surface summer Chl *a* and POC concentrations could also have been altered by the change in phytoplankton morphology, which is known to affect marine particles' Inherent Optical Properties (IOP), and therefore the assessment of Chl *a* and POC concentrations from space (Clavano et al. 2007; Stramski et al. 2008; Stemmann and Boss 2012).

Finally, increasing temperature during the NPMHWs also had a high socio-economic cost, with the closure of the North Pacific cod (*G. macrocephalus*) fishery in the Gulf of Alaska in 2019–2020 (Barbeaux et al. 2020). Shift in phytoplankton composition (e.g., from diatoms to dinoflagellates) could alter copepod nutritional quality and therefore the growth and survival of the fish larvae that feed on them (Beaugrand et al. 2003a; Copeman and Laurel 2010). In that case, our results may suggest that the shift in phytoplankton summer abundance and morphology could also be related to the decline in cod population, through a bottom-up effect that may decrease trophic transfer efficiency (Arimitsu et al. 2021). However, in the Gulf of Alaska, cod larval habitat suitability has been found to be mainly related to the interannual fluctuations in temperature that regulate larval yolk reserve and metabolic demands (Barbeaux et al. 2020; Laurel et al. 2021). Pacific cod eggs also have a narrow thermal tolerance, which makes the early life stages of this fish highly sensitive to temperature changes (Laurel et al. 2023). Hence, although the decline in trophic transfer efficiency could have acted as an additional stressor, cod decline is very unlikely to have been caused by the shift in phytoplankton abundance and morphology (i.e., bottom-up mechanism) but is rather related to the effect of higher temperature on cod metabolic rate (Barbeaux et al. 2020). Cod decline can also be related to the compound extreme events (i.e., the co-occurrence of two or more extreme events in time and space) that occurred above the Gulf of Alaska continental shelves (i.e., increasing temperature and acidity associated with low oxygen), which may explain why their populations have not recovered after the return to pre-heatwave conditions (Hauri et al. 2024).

Conclusion

Consequences of MHWs on biological systems are well documented, mostly because of their high socio-economic impacts (Smith et al. 2021, 2023). Here, our results showed for the first time a previously unknown outcome of this phenomenon, i.e., a shift in phytoplankton cell size and shape with an increase in summer abundance of large prolate taxa. Although many mechanisms can be invoked to explain this alteration (e.g., changes in grazing pressure), our results demonstrated that this increase was induced by warming temperature and declining nitrate. Furthermore, the changes in phytoplankton mean cell carbon content and shape have likely impacted the carbon cycle, due to changes in cells sinking velocity (Padisak et al. 2003; Naselli-Flores et al. 2021), as shown by the observed decrease in surface Chl *a* and POC concentrations during these events. The increase in smaller cells (Fig. 5d) with a lower Chl *a* content (Hillebrand et al. 2022) as well as the potential changes in phytoplankton intracellular pigmentation (Behrenfeld et al. 2016) may also have impacted surface Chl *a* and POC concentrations and decreased the potential biological carbon pump. Hence, MHWs have multiple ways of impacting phytoplankton community and related ecosystem services.

Author Contributions

Loïck Kléparski, Clare Ostle, Sonia D. Batten, and Nicolas Djeghri designed the study. Loïck Kléparski ran the numerical analyses and wrote the first draft of the manuscript. Claudine Hauri and Rémi Pagès provided the Northern Alaska Gyre Oscillation index. Suzanne Strom provided the Seward line data. All authors provided critical feedback, helped shape the analyses, and contributed to the writing of the original and revised manuscript.

Acknowledgments

The authors would like to thank the owners and crews that have towed the CPRs on a voluntary basis for over 20 years in the North Pacific Ocean. We are also grateful to Grégory Beaugrand for making insightful comments that greatly improved the manuscript. The North Pacific CPR survey is supported by a consortium of funders coordinated by the North Pacific Marine Science Organization (PICES) and comprising the North Pacific Research Board (NPRB), Exxon Valdez Oil Spill Trustee Council (EVOSTC) through Gulf Watch Alaska (GWA), Canadian Department of Fisheries and Oceans (DFO) and the Marine Biological Association of the UK. Claudine Hauri and Rémi Pagès acknowledge support from the North

Pacific Research Board (NPRB 2109) and National Science Foundation (OCE-1656070).

Conflicts of Interest

None declared.

References

Amaya, D. J., A. J. Miller, S. P. Xie, and Y. Kosaka. 2020. "Physical Drivers of the Summer 2019 North Pacific Marine Heatwave." *Nature Communications* 11: 1903. https://doi.org/10.1038/s41467-020-15820-w.

Arguedas-Leiva, J. A., J. Słomka, C. C. Lalescu, R. Stocker, and M. Wilczek. 2022. "Elongation Enhances Encounter Rates Between Phytoplankton in Turbulence." *Proceedings. National Academy of Sciences. United States of America* 119: e2203191119. https://doi.org/10.1073/pnas.2203191119.

Arimitsu, M. L., J. F. Piatt, S. Hatch, et al. 2021. "Heatwave-Induced Synchrony Within Forage Fish Portfolio Disrupts Energy Flow to Top Pelagic Predators." *Global Change Biology* 27: 1859–1878. https://doi.org/10.1111/gcb.15556.

Atkinson, D., B. J. Ciotti, and J. S. Montagnes. 2003. "Protists Decrease in Size Linearly With Temperature: ca. 2.5%° C−1." *Proceedings of the Royal Society B: Biological Sciences* 270: 2605–2611. https://doi.org/10.1098/rspb.2003.2538.

Barbeaux, S. J., K. Holsman, and S. Zador. 2020. "Marine Heatwave Stress Test of Ecosystem-Based Fisheries Management in the Gulf of Alaska Pacific Cod Fishery." *Frontiers in Marine Science* 7: 703. https://doi.org/10.3389/fmars.2020.00703.

Barkhordarian, A., D. M. Nielsen, and J. Baehr. 2022. "Recent Marine Heatwaves in the North Pacific Warming Pool Can be Attributed to Rising Atmospheric Levels of Greenhouse Gases." *Communications Earth & Environment* 3: 131. https://doi.org/10.1038/s43247-022-00461-2.

Barton, A. D., Z. V. Finkel, B. A. Ward, D. G. Johns, and M. J. Follows. 2013. "On the Roles of Cell Size and Trophic Strategy in North Atlantic Diatom and Dinoflagellate Communities." *Limnology and Oceanography* 58: 254–266. https://doi.org/10.4319/lo.2013.58.1.0254.

Batten, S. D., R. Clark, J. Flinkman, et al. 2003. "CPR Sampling: The Technical Background, Materials and Methods, Consistency and Comparability." *Progress in Oceanography* 58: 193–215. https://doi.org/10.1016/j.pocean.2003.08.004.

Batten, S. D., C. Ostle, P. Hélaouët, and A. W. Walne. 2022. "Responses of Gulf of Alaska Plankton Communities to a Marine Heat Wave." *Deep Sea Research Part II: Topical Studies in Oceanography* 195: 105002. https://doi.org/10.1016/j.dsr2.2021.105002.

Batten, S. D., D. E. Raitsos, S. Danielson, R. R. Hopcroft, K. Coyle, and A. McQuatters-Gollop. 2018. "Interannual Variability in Lower Trophic Levels on the Alaskan Shelf." *Deep Sea Research Part II: Topical Studies in Oceanography* 147: 58–68. https://doi.org/10.1016/j.dsr2.2017.04.023.

Beaugrand, G., K. M. Brander, J. A. Lindley, S. Souissi, and P. C. Reid. 2003*a*. "Plankton Effect on Cod Recruitment in the North Sea." *Nature* 426: 661–664. https://doi.org/10.1038/nature02164.

Beaugrand, G., F. Ibañez, and J. A. Lindley. 2003*b*. "An Overview of Statistical Methods Applied to CPR Data." *Progress in Oceanography* 58: 235–262. https://doi.org/10.1016/j.pocean.2003.08.006.

Behrenfeld, M. J., E. S. Boss, D. A. Siegel, and D. M. Shea. 2005. "Carbon-Based Ocean Productivity and Phytoplankton Physiology From Space." *Global Biogeochemical Cycles* 19: GB1006. https://doi.org/10.1029/2004GB002299.

Behrenfeld, M. J., R. T. O'Malley, D. A. Siegel, et al. 2006. "Climate-Driven Trends in Contemporary Ocean Productivity." *Nature* 444: 752–755. https://doi.org/10.1038/nature05317.

Behrenfeld, M. J., R. T. O'Malley, E. S. Boss, et al. 2016. "Revaluating Ocean Warming Impacts on Global Phytoplankton." *Nature Climate Change* 6: 323–330. https://doi.org/10.1038/nclimate2838.

Bond, N. A., M. F. Cronin, H. Freeland, and N. Mantua. 2015. "Causes and Impacts of the 2014 Warm Anomaly in the NE Pacific." *Geophysical Research Letters* 42: 3414–3420. https://doi.org/10.1002/2015GL063306.

Bopp, L., O. Aumont, P. Cadule, S. Alvain, and M. Gehlen. 2005. "Response of Diatoms Distribution to Global Warming and Potential Implications: A Global Model Study." *Geophysical Research Letters* 32: L19606. https://doi.org/10.1029/2005GL023653.

Boyce, D. G., M. R. Lewis, and B. Worm. 2010. "Global Phytoplankton Decline Over the Past Century." *Nature* 466: 591–596. https://doi.org/10.1038/nature09268.

Cai, W., S. Borlace, M. Lengaigne, et al. 2014. "Increasing Frequency of Extreme El Niño Events Due to Greenhouse Warming." *Nature Climate Change* 4: 111–116. https://doi.org/10.1038/nclimate2100.

Clavano, W. R., E. S. Boss, and L. Karp-Boss. 2007. "Inherent Optical Properties of Non-Spherical Marine-Like Particules—From Theory to Observation." *Oceanography and Marine Biology. Annual Review* 45: 1–38.

Clifton, W., R. N. Bearon, and M. A. Bees. 2018. "Enhanced Sedimentation of Elongated Plankton in Simple Flows." *IMA Journal of Applied Mathematics* 83: 743–766. https://doi.org/10.1093/imamat/hxy024.

Cohen, J. 2022. Shifts in Microbial Community Composition During the 2019 Pacific Marine Heatwave in the Northern Gulf of Alaska. University of Alaska Fairbanks.

Colebrook, J. M. 1984. "Continuous Plankton Records: Relationships Between Species of Phytoplankton and Zooplankton in the Seasonal Cycle." *Marine Biology* 83: 313–323. https://doi.org/10.1007/BF00397464.

Colebrook, J. M. 1986. "Environmental Influences on Long-Term Variability in Marine Plankton." *Hydrobiologia* 142: 309–325. https://doi.org/10.1007/BF00026767.

Copeman, L. A., and B. J. Laurel. 2010. "Experimental Evidence of Fatty Acid Limited Growth and Survival in Pacific Cod Larvae." *Marine Ecology Progress Series* 412: 259–272. https://doi.org/10.3354/meps08661.

Di Lorenzo, E., and N. Mantua. 2016. "Multi-Year Persistence of the 2014/15 North Pacific Marine Heatwave." *Nature Climate Change* 6: 1042–1047. https://doi.org/10.1038/nclimate3082.

Duke, P. J., R. C. Hamme, D. Ianson, et al. 2023. "Estimating Marine Carbon Uptake in the Northeast Pacific Using a Neural Network Approach." *Biogeosciences* 20: 3919–3941. https://doi.org/10.5194/bg-20-3919-2023.

Edwards, K. F., M. K. Thomas, C. A. Klausmeier, and E. Litchman. 2016. "Phytoplankton Growth and the Interaction of Light and Temperature: A Synthesis at the Species and Community Level." *Limnology and Oceanography* 61: 1232–1244. https://doi.org/10.1002/lno.10282.

Evers-King, H., V. Martinez-Vicente, R. J. W. Brewin, et al. 2017. "Validation and Intercomparison of Ocean Color Algorithms for Estimating Particulate Organic Carbon in the Oceans." *Frontiers in Marine Science* 4: 251. https://doi.org/10.3389/fmars.2017.00251.

Hauri, C., R. Pagès, K. Hedstrom, et al. 2024. "More than Marine Heatwaves: A New Regime of Heat, Acidity, and Low Oxygen Compound Extrem Events in the Gulf of Alaska." *AGU Advances* 5: e2023AV001039. https://doi.org/10.1029/2023AV001039.

Hauri, C., R. Pagès, A. M. P. McDonnell, et al. 2021. "Modulation of Ocean Acidification by Decadal Climate Variability in the Gulf of Alaska." *Communications Earth & Environment* 2: 191. https://doi.org/10.1038/s43247-021-00254-z.

Henson, S. A., R. S. Lampitt, and D. Johns. 2012. "Variability in Phytoplankton Community Structure in Response to the North Atlantic Oscillation and Implications for Organic Carbon Flux." *Limnology and Oceanography* 57: 1591–1601. https://doi.org/10.4319/lo.2012.57.6.1591.

Henson, S. A., C. Laufkötter, S. Leung, S. L. C. Giering, H. I. Palevsky, and E. L. Cavan. 2022. "Uncertain Response of Ocean Biological Carbon Export in a Changing World." *Nature Geoscience* 15: 248–254. https://doi.org/10.1038/s41561-022-00927-0.

Henson, S. A., F. Le Moigne, and S. Giering. 2019. "Drivers of Carbon Export Efficiency in the Global Ocean." *Global Biogeochemical Cycles* 33: 891–903. https://doi.org/10.1029/2018GB006158.

Hillebrand, H., E. Acevedo-Trejos, S. D. Moorthi, et al. 2022. "Cell Size as Driver and Sentinel of Phytoplankton Community Structure and Functioning." *Functional Ecology* 36: 276–293. https://doi.org/10.1111/1365-2435.13986.

Hillebrand, H., C. D. Dürselen, D. Kirschtel, U. Pollingher, and T. Zohary. 1999. "Biovolume Calculation for Pelagic and Benthic Microalgae." *Journal of Phycology* 35: 403–424. https://doi.org/10.1046/j.1529-8817.1999.3520403.x.

Hutchinson, G. E. 1957. "Concluding Remarks." *Cold Spring Harbor Symposia on Quantitative Biology* 22: 415–427. https://doi.org/10.1101/SQB.1957.022.01.039.

IPCC. 2019. "Annex I: Glossary." In IPCC Special Report on the Ocean and Cryosphere in a Changing Climate, edited by N. M. Weyer, D. C. Pörtner, D. C. Roberts, et al., 677–702. New York: Cambridge University Press.

Jonas, T. D., A. W. Walne, G. Beaugrand, L. Gregory, and G. C. Hays. 2004. "The Volume of Water Filtered by a Continuous Plankton Recorder Sample: The Effect of Ship Speed." *Journal of Plankton Research* 26: 1499–1506. https://doi.org/10.1093/plankt/fbh137.

Jones, T., J. K. Parrish, J. Lindsey, et al. 2023. "Marine Bird Mass Mortality Events as an Indicator of the Impacts of Ocean Warming." *Marine Ecology Progress Series: HEAT* 737: 161–181. https://doi.org/10.3354/meps14330.

Karp-Boss, L., and E. S. Boss. 2016. "The Elongated, the Squat and the Spherical: Selective Pressures for Phytoplankton Shape." In Aquatic Microbial Ecology and Biogeochemistry: A Dual Perspective, edited by P. M. Glibert and T. M. Kana, 25–34. Cham: Springer International Publishing.

Kemp, A. E. S., and T. A. Villareal. 2013. "High Diatom Production and Export in Stratified Waters—A Potential Negative Feedback to Global Warming." *Progress in Oceanography* 119: 4–23. https://doi.org/10.1016/j.pocean.2013.06.004.

Kléparski, L., G. Beaugrand, M. Edwards, and C. Ostle. 2023. "Phytoplankton Life Strategies, Phenological Shifts and Climate Change in the North Atlantic Ocean From 1850–2100." *Global Change Biology* 29: 3833–3849. https://doi.org/10.1111/gcb.16709.

Kléparski, L., G. Beaugrand, M. Edwards, et al. 2022. "Morphological Traits, Niche-Environment Interaction and Temporal Changes in Diatoms." *Progress in Oceanography* 201: 102747. https://doi.org/10.1016/j.pocean.2022.102747.

Laurel, B. J., M. E. Hunsicker, L. Ciannelli, et al. 2021. "Regional Warming Exacerbates Match/Mismatch Vulnerability for Cod Larvae in Alaska." *Progress in Oceanography* 193: 102555. https://doi.org/10.1016/j.pocean.2021.102555.

Laurel, B. J., A. Abookire, S. J. Barbeaux, et al. 2023. "Pacific Cod in the Anthropocene: An Early Life History Perspective Under Changing Thermal Habitats." *Fisheries Oceanography* 23: 959–978. https://doi.org/10.1111/faf.12779.

Leblanc, K., J. Arístegui, L. Armand, et al. 2012. "A Global Diatom Database—Abundance, Biovolume and Biomass in the World Ocean." *Earth System Science Data* 4: 149–165. https://doi.org/10.5194/essd-4-149-2012.

Legendre, P., and L. Legendre. 1998. Numerical Ecology. New York: Elsevier.

Lewandowska, A., H. Hillebrand, K. Lengfellner, and U. Sommer. 2014. "Temperature Effects on Phytoplankton Diversity—The Zooplankton Link." *Journal of Sea Research* 85: 359–364. https://doi.org/10.1016/j.seares.2013.07.003.

Lewandowska, A., and U. Sommer. 2010. "Climate Change and the Spring Bloom: A Mesocosm Study on the Influence of Light and Temperature on Phytoplankton and Mesozooplankton." *Marine Ecology Progress Series* 405: 101–111. https://doi.org/10.3354/meps08520.

Litchman, E., and C. A. Klausmeier. 2008. "Trait-Based Community Ecology of Phytoplankton." *Annual Review of Ecology, Evolution, and Systematics* 39: 615–639. https://doi.org/10.1146/annurev.ecolsys.39.110707.173549.

Longhurst, A. 1998. Ecological Geography of the Sea. New York: Academic Press.

Lopes, C., M. Kucera, and A. C. Mix. 2015. "Climate Change Decouples Oceanic Primary and Export Productivity and Organic Carbon Burial." *Proceedings. National Academy of Sciences. United States of America* 112: 332–335. https://doi.org/10.1073/pnas.1410480111.

Marinov, I., S. C. Doney, and I. D. Lima. 2010. "Response of Ocean Phytoplankton Community Structure to Climate Change Over the 21st Century: Partitioning the Effects of Nutrients, Temperature and Light." *Biogeosciences* 7: 3941–3959. https://doi.org/10.5194/bg-7-3941-2010.

Marsay, C. M., R. J. Sanders, S. A. Henson, K. Pabortsava, E. P. Achterberg, and R. Lampitt. 2015. "Attenuation of Sinking Particulate Organic Carbon Flux Through the Mesopelagic Ocean." *Proceedings. National Academy of Sciences. United States of America* 112: 1089–1094. https://doi.org/10.1073/pnas.1415311112.

Martin, J. H., R. M. Gordon, S. Fitzwater, and W. W. Broenkow. 1989. "VERTEX: Phytoplankton/Iron Studies in the Gulf of Alaska." *Deep Sea Research Part I: Oceanographic Research Papers* 36: 649–680. https://doi.org/10.1016/0198-0149(89)90144-1.

Miller, C. B. 2004. Biological Oceanography. Malden: Blackwell Science.

Mouw, C. B., A. Barnett, G. A. McKinley, L. Gloege, and D. Pilcher. 2016. "Phytoplankton Size Impact on Export Flux in the Global Ocean." *Global Biogeochemical Cycles* 30: 1542–1562. https://doi.org/10.1002/2015GB005355.

Naselli-Flores, L., and R. Barone. 2011. "Invited Review—Fight on Plankton! Or, Phytoplankton Shape and Size as Adaptive Tools to Get Ahead in the Struggle for Life." *Cryptogamie, Algologie* 32: 157–204. https://doi.org/10.7872/crya.v32.iss2.2011.157.

Naselli-Flores, L., T. Zohary, and J. Padisák. 2021. "Life in Suspension and Its Impact on Phytoplankton Morphology: An Homage to Colin S. Reynolds." *Hydrobiologia* 848: 7–30. https://doi.org/10.1007/s10750-020-04217-x.

O'Daly, S. H., G. M. M. Hennon, T. B. Kelly, S. L. Strom, and A. M. P. McDonnell. 2024. "Strong and Efficient Summertime Carbon Export Driven by Aggregation Processes in a Subarctic Coastal Ecosystem." *Limnology and Oceanography* 9999: 1–17. https://doi.org/10.1002/lno.12561.

Oliver, E. C. J., J. A. Benthuysen, S. Darmaraki, et al. 2021. "Marine Heatwaves." *Annual Review of Marine Science* 13, no. 313: 342. https://doi.org/10.1146/annurev-marine-032720-095144.

Padfield, D., A. Buckling, R. Warfield, C. Lowe, and G. Yvon-Durocher. 2018. "Linking Phytoplankton Community Metabolism to the Individual Size Distribution." *Ecology Letters* 21: 1152–1161. https://doi.org/10.1111/ele.13082.

Padisak, J., E. Soroczki-Pinter, and Z. Rezner. 2003. "Sinking Properties of Some Phytoplankton Shapes and the Relation of Form Resistance to Morphological Diversity of Plankton—An Experimental Study." *Hydrobiologia* 500: 243–257. https://doi.org/10.1023/A:1024613001147.

Pahlow, M., U. Riebesell, and D. A. Wolf-Gladrow. 1997. "Impact of Cell Shape and Chain Formation on Nutrient Acquisition by Marine Diatoms." *Limnology and Oceanography* 42: 1660–1672. https://doi.org/10.4319/lo.1997.42.8.1660.

Peña, M. A., N. Nemcek, and M. Robert. 2019. "Phytoplankton Responses to the 2014–2016 Warming Anomaly in the Northeast Subarctic Pacific Ocean." *Limnology and Oceanography* 64: 515–525. https://doi.org/10.1002/lno.11056.

Peter, K. H., and U. Sommer. 2012. "Phytoplankton Cell Size: Intra and Interspecific Effects of Warming and Grazing." *PLoS One* 7: e49632. https://doi.org/10.1371/journal.pone.0049632.

Praetorius, S. K., A. C. Mix, M. H. Walczak, M. D. Wolhowe, J. A. Addison, and F. G. Prahl. 2015. "North Pacific Deglacial Hypoxic Events Linked to Abrupt Ocean Warming." *Nature* 527: 362–366. https://doi.org/10.1038/nature15753.

Richardson, A. J., A. W. Walne, A. W. G. John, et al. 2006. "Using Continuous Plankton Recorder Data." *Progress in Oceanography* 68: 27–74. https://doi.org/10.1016/j.pocean.2005.09.011.

Ryabov, A., O. Kerimoglu, E. Litchman, et al. 2021. "Shape Matters: The Relationship between Cell Geometry and Diversity in Phytoplankton." *Ecology Letters* 24: 847–861. https://doi.org/10.1111/ele.13680.

Scannell, H. A., G. C. Johnson, L. Thompson, J. M. Lyman, and S. C. Riser. 2020. "Subsurface Evolution and Persistence of Marine Heatwaves in the Northeast Pacific." *Geophysical Research Letters* 47: e2020GL090548. https://doi.org/10.1029/2020GL090548.

Smayda, T. 1970. "The Suspension and Sinking of Phytoplankton in the Sea." *Oceanography and Marine Biology. Annual Review* 8: 353–414.

Smetacek, V. 2001. "A Watery Arms Race." *Nature* 411: 745. https://doi.org/10.1038/35081210.

Smith, K. E., M. T. Burrows, A. J. Hobday, et al. 2021. "Socioeconomic Impacts of Marine Heatwaves: Global Issues and Opportunities." *Science* 374: eabj3593. https://doi.org/10.1126/science.abj3593.

Smith, K. E., M. T. Burrows, A. J. Hobday, et al. 2023. "Biological Impacts of Marine Heatwaves." *Annual Review of Marine Science* 15: 119–145. https://doi.org/10.1146/annurev-marine-032122-121437.

Stemmann, L., and E. S. Boss. 2012. "Plankton and Particle Size and Packaging: From Determining Optical Properties

to Driving the Biological Pump." *Annual Review of Marine Science* 4: 263–290. https://doi.org/10.1146/annurev-marine-120710-100853.

Stramski, D., R. A. Reynolds, M. Babin, et al. 2008. "Relationships Between the Surface Concentration of Particulate Organic Carbon and Optical Properties in the Eastern South Pacific and Eastern Atlantic Oceans." *Biogeosciences* 5: 171–201. https://doi.org/10.5194/bg-5-171-2008.

Strom, S. L., M. Brady Olson, E. L. Macri, and C. W. Mord. 2006. "Cross-Shelf Gradients in Phytoplankton Community Structure, Nutrient Utilization, and Growth Rate in the Coastal Gulf of Alaska." *Marine Ecology Progress Series* 328: 75–92. https://doi.org/10.3354/meps328075.

Strom, S. L., K. A. Fredrickson, and K. J. Bright. 2016. "Spring Phytoplankton in the Eastern Coastal Gulf of Alaska: Photosynthesis and Production During High and Low Bloom Years." *Deep Sea Research Part II: Topical Studies in Oceanography* 132: 107–121. https://doi.org/10.1016/j.dsr2.2015.05.003.

Sun, J., and D. Liu. 2003. "Geometric Models for Calculating Cell Biovolume and Surface Area for Phytoplankton." *Journal of Plankton Research* 25: 1331–1346. https://doi.org/10.1093/plankt/fbg096.

Suryan, R. M., M. L. Arimitsu, H. A. Coletti, et al. 2021. "Ecosystem Response Persists after a Prolonged Marine Heatwave." *Scientific Reports* 11: 6235. https://doi.org/10.1038/s41598-021-83818-5.

Toseland, A., S. J. Daines, J. R. Clark, et al. 2013. "The Impact of Temperature on Marine Phytoplankton Resource Allocation and Metabolism." *Nature Climate Change* 3: 979–984. https://doi.org/10.1038/nclimate1989.

Wackernagel, H. 1995. Multivariate Geostatistics. An Introduction With Applications. Berlin: Springer-Verlag.

Ward, B. A., and M. J. Follows. 2016. "Marine Mixotrophy Increases Trophic Transfer Efficiency, Mean Organism Size, and Vertical Carbon Flux." *Proceedings. National Academy of Sciences. United States of America* 113: 2958–2963. https://doi.org/10.1073/pnas.1517118113.

Wyatt, A. M., L. Resplandy, and A. Marchetti. 2022. "Ecosystem Impacts of Marine Heat Waves in the Northeast Pacific." *Biogeosciences* 19: 5689–5705. https://doi.org/10.5194/bg-19-5689-2022.

Yu, J., X. Wang, H. Fan, and R. H. Zhang. 2019. "Impacts of Physical and Biological Processes on Spatial and Temporal Variability of Particulate Organic Carbon in the North Pacific Ocean during 2003–2017." *Scientific Reports* 9: 16493. https://doi.org/10.1038/s41598-019-53025-4.

Yvon-Durocher, G., J. M. Montoya, M. Trimmer, and G. Woodward. 2011. "Warming Alters the Size Spectrum and Shifts the Distribution of Biomass in Freshwater Ecosystems." *Global Change Biology* 17: 1681–1694. https://doi.org/10.1111/j.1365-2486.2010.02321.x.

Supporting Information

Additional Supporting Information may be found in the online version of this article.

Submitted 14 January 2025
Revised 28 April 2025
Accepted 09 July 2025